



# Epoxide ring opening with alcohols using heterogeneous Lewis acid catalysts: Regioselectivity and mechanism



Nitish Deshpande<sup>a</sup>, Aamena Parulkar<sup>a</sup>, Rutuja Joshi<sup>a</sup>, Brian Diep<sup>a</sup>, Ambarish Kulkarni<sup>b</sup>, Nicholas A. Brunelli<sup>a,\*</sup>

<sup>a</sup> Ohio State University, William G. Lowrie Department of Chemical and Biomolecular Engineering, 151 W. Woodruff Ave., Columbus, OH 43210, United States

<sup>b</sup> University of California Davis, Department of Chemical Engineering, 1 Shields Avenue, Davis, CA 95616, United States

## ARTICLE INFO

### Article history:

Received 11 September 2018

Revised 29 November 2018

Accepted 30 November 2018

Available online 20 December 2018

### Keywords:

Lewis acidic zeolites

Epoxide ring opening

Sn-Beta

Cluster calculations

Regioselectivity

## ABSTRACT

Lewis acidic catalytic materials are investigated for the regioselective ring opening of epoxides with alcohols. For ring opening epichlorohydrin with methanol, the catalytic activity shows a strong dependence on the type of support and Lewis acidic species used. While Sn-SBA-15 is catalytically active, significantly higher catalytic activity can be achieved with hydrothermally synthesized zeolites of which Sn-Beta is 6 and 7 times more active than Zr-Beta or Hf-Beta, respectively. Sn-Beta is determined to be more active and more regioselective for epoxide ring opening of epichlorohydrin with methanol than Al-Beta. For Sn-Beta, the activation energy for the reaction between epichlorohydrin and methanol is determined to be  $53 \pm 7$  kJ mol<sup>-1</sup>. For epichlorohydrin, the activation energy barrier and experimentally observed regioselectivity are found using DFT to be consistent with a concerted reaction mechanism involving activation of the epoxide on an alcohol adsorbed on the catalytic site and nucleophilic attack by a second alcohol. The epoxide is shown to impact the regioselectivity and the mechanism since isobutylene oxide is selectively ring opened by methanol to form the terminal alcohol. DFT calculations indicate the mechanism for isobutylene ring opening involves epoxide activation and ring opening on an alcohol adsorbed onto the catalytic site. Finally, catalyst reuse testing indicates that Sn-Beta can be used for multiple reactions with no decrease in activity and limited to no leaching of the tin site, demonstrating Sn-Beta is a promising catalytic material for epoxide ring opening reactions with alcohols.

© 2018 Elsevier Inc. All rights reserved.

## 1. Introduction

Epoxides are versatile chemical intermediates that can be transformed to produce many products. Indeed, epoxides are commonly transformed through ring opening reactions with different nucleophiles such as water [1,2], alcohols [3–12], amines [8,13–16], and other substrates [17–20] to produce a broad range of bifunctional products. In particular, alcohol ring opening products are commonly encountered in compounds relevant to the pharmaceutical and solvents industry [21,22]. The key challenge for these reactions is selectivity, because of the tendency of epoxides – especially terminal epoxides like epichlorohydrin – to polymerize [23]. This necessitates the reaction be carried out under mild conditions. Additional selectivity challenges result from the fact that the ring opening can occur with attack of the nucleophile on the carbon in the 1 or 2 position (Scheme 1). Thus, it is important to under-

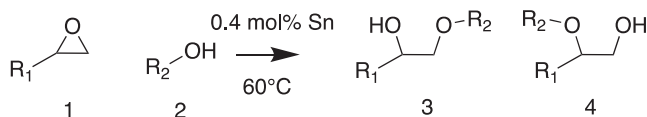
stand factors controlling catalytic activity and selectivity for these reactions.

The ring opening reactions are commonly catalyzed using strong acids [16,24,25], Lewis bases [26], or Lewis acids [4,10,27–30]. While strong acids are important industrially, they tend to result in low regioselectivity for the epoxide ring opening with alcohols [16,24]. Recently, Lewis basic amines were investigated for ring opening with phenolic nucleophiles, demonstrating that immobilized tertiary amines could be used as heterogeneous catalysts [26]. These catalysts were incompatible with substrates such as epichlorohydrin since the nucleophile can displace the chloro group, affording a low chemoselectivity. The importance of this reaction has spurred investigations into using Lewis acids as catalysts for these reactions. While alcohols are weak Lewis bases that can adsorb on Lewis acidic sites, powerful catalysts such as cobalt-salen and cobalt-porphyrin were demonstrated to be highly active and could be made into a heterogeneous catalyst [10,28,29,31]. These catalysts tended to deactivate through loss of a counterion that maintained the cobalt in a +3 oxidation state, which is the catalytically active form of cobalt. Additional catalysts include

\* Corresponding author.

E-mail address: [brunelli.2@osu.edu](mailto:brunelli.2@osu.edu) (N.A. Brunelli).

@OSUChemEProfBru (N.A. Brunelli)



**Scheme 1.** Epoxide ring opening reaction converting a terminal epoxide (1) with an alcohol (2) using a Lewis acidic catalyst (0.4 mol% Lewis acid - mostly Sn - and 60 °C is used) to produce beta alkoxy alcohols with either a terminal ether (3) or a secondary ether (4).

metal organic frameworks such as NU-1000, MOF-808, and Fe(BTC) [12,27]. NU-1000 and MOF-808 can be activated for this reaction through creating defects in the material that may limit stability. Fe(BTC) can catalyze the reaction without any such activation, but the crystal structure changes upon catalytic testing that could impact catalyst reuse. Therefore, it is desirable to find alternative Lewis acidic catalysts for this reaction that maintain activity upon catalytic material reuse.

Lewis acidic Zr, Hf, or Sn substituted into the silica framework offer another alternate class of important heterogeneous Lewis acidic catalysts. These materials have higher thermal stability than MOFs, making them a robust catalytic support. Indeed, microporous Sn-Beta and Sn-MFI, and mesoporous Sn-SBA-15 have been utilized for numerous reactions as Lewis acid catalysts [32–35]. While the Lewis acid catalyzed epoxide ring opening reaction with amines [13] and water [1] has been studied, similar studies have not examined epoxide ring opening with alcohols.

In this work, a suite of catalytic supports are examined that contain Lewis acidic catalytic sites, ranging from mesoporous Sn-SBA-15 [13] to zeolite Sn-Beta. The catalytic activity is investigated for these different materials through studying the epoxide ring opening of epichlorohydrin with methanol as a standard reaction. After identifying a highly active catalyst, the scope of the reaction is tested through reacting a range of alcohols and epoxides to determine the effect of substrate on the catalytic activity and regioselectivity. The heterogeneous catalyst is further tested in recycle experiments to determine the reusability of the catalytic materials. Cluster calculations are utilized to examine the potential different catalytic pathways, allowing differentiation between four potential mechanisms. Overall, the work demonstrates a range of catalytic materials that are highly active and selective for the epoxide ring opening reaction.

## 2. Experimental methods

### 2.1. Material syntheses

#### 2.1.1. Co-condensation synthesis of mesoporous silica with tin (Co-Sn-SBA-15)

Co-Sn-SBA-15 is synthesized using a procedure reported in literature [36]. Briefly, a mixture is made of P-123 and DI water with HCl. The solution is stirred at 40 °C to dissolve P-123 before adding tetraethylorthosilicate (TEOS) and tin tetrachloride pentahydrate (SnCl<sub>4</sub>·5H<sub>2</sub>O) and allowing the mixture to stir for 24 h. The contents are transferred to a 44 mL Teflon-lined acid-digestion vessel (Parr Inst. Comp.) and aged at 100 °C under static conditions for 24 h. After cooling to room temperature, the reaction mixture is filtered and washed with DI water. Recovered solids are calcined under flowing air at 550 °C for 12 h.

#### 2.1.2. Post-synthetic incorporation of mesoporous silica with tin (PS-Sn-SBA-15)

Pure silica SBA-15 is synthesized using a procedure reported in literature [37,38]. After calcination, the pure silica SBA-15 is dried under vacuum overnight at 140 °C. The material is suspended in

dry tetrahydrofuran (THF) before addition of SnCl<sub>4</sub>·5H<sub>2</sub>O in THF (Si:Sn of 200:1). After stirring for 24 h, the mixture is rotovapped to dryness before calcining under air at 550 °C.

### 2.1.3. Hydrothermal synthesis of Lewis acidic zeolite Beta

The synthesis of Sn-Beta is achieved through scaling up the procedure used in previous work [32,34,39] to produce larger quantities of material. Briefly, a mixture is made of TEOS and tetraethyl ammonium hydroxide (TEAOH; 35 wt% aqueous solution) before addition of SnCl<sub>4</sub>·5H<sub>2</sub>O. The mixture is allowed to hydrolyze overnight before concentrating using a rotovap, transferring to a Teflon-lined 200 mL acid-digestion vessel (Parr Inst. Comp.), and adding aqueous hydrofluoric acid (HF), and 350 mg (5 wt%) of calcined Si-Beta seeds. The final gel composition is 1 SiO<sub>2</sub>/ 0.005 Sn/ 0.54 F<sup>-</sup>/ 0.54 TEA/ 7.5 H<sub>2</sub>O (Si:Sn of 200:1). The acid digestion vessel is sealed and placed in a preheated oven at 140 °C with rotation at 35 RPM for 30 days. Materials formed are filtered and washed with 1 L DI water before drying and calcining in air at 550 °C. A similar procedure is used for Zr-Beta and Hf-Beta with the modification that the materials are produced on the 0.9 g scale by scaling the amounts of each component down by a factor of eight and substituting the tin source with either zirconyl chloride (ZrOCl<sub>2</sub>) and hafnium tetrachloride (HfCl<sub>4</sub>) for Zr-Beta and Hf-Beta, respectively.

### 2.1.4. Synthesis of Sn-MFI

A mixture is made of 0.177 g SnCl<sub>4</sub>·5H<sub>2</sub>O and 6.75 g DI water in a 200 mL Teflon-lined acid-digestion vessel (Parr Inst. Comp.). To this, TEOS (21 g) is slowly added to this solution under stirring (magnetic Teflon stir bar). After 30 min, a mixture of 22.25 g tetrapropylammonium hydroxide (40% by wt.) and 22.25 g DI water is added to this mixture slowly. After 1 h of mixing, 18.9 g DI water is added, and the mixture is stirred for 30 min. The stir bar is removed, the reactor sealed and placed in a pre-heated oven at 160 °C under static conditions. After 5 days, the reactor is cooled under flowing water, and the contents are centrifuged and washed with DI water three times before drying at 80 °C overnight. The dried material is calcined in air using the same conditions described for Sn-Beta.

## 2.2. Material characterization

The materials are characterized using a battery of standard techniques, including powder X-ray diffraction (PXRD), nitrogen physisorption, scanning electron microscopy (SEM), diffuse reflectance ultraviolet-visible spectroscopy (DRUVS), and diffuse reflectance Fourier Transform Infrared spectroscopy (DRIFTS). PXRD is recorded using a Bruker PXRD in standard reflection mode using monochromatic Cu K<sub>α1</sub> radiation (λ = 1.54 Å) at 40 kV and 50 mA to demonstrate the crystallinity of zeolites. Nitrogen physisorption is measured using a Micromeritics 3Flex surface characterization analyzer after degassing at 140 °C under vacuum to investigate the textural properties (e.g., pore volume) of the materials. DRUVS is collected using an Evolution 300 UV-Vis spectrometer with a resolution of 2 nm at a scan rate of 10 nm·s<sup>-1</sup> using pure silica analogues of materials analyzed as a baseline to identify tin oxide (SnO<sub>2</sub>) formation [40]. DRIFTS is performed using a Nicolet iS50 spectrometer equipped with a MCT-A liquid nitrogen cooled detector (32 scans at 2 cm<sup>-1</sup> resolutions are collected for every spectrum using the bare material (without CD<sub>3</sub>CN exposure) as the background reference) using a Harrick high temperature reaction chamber with ZnSe windows. After degassing the material at 500 °C under a flow of nitrogen, deuterated acetonitrile is adsorbed on the material at room temperature, and a spectra is recorded to identify of open and closed sites [41]. SEM is performed on a FEI Nova 400 NanoSEM scanning electron microscope on samples prepared by dispersing the material (2 mg in 100 μL of methanol)

on carbon conductive tape and drying the sample before sputter coating at 17 mA for 60 s with a gold–palladium alloy using Cressington 108 Sputter coater or an 8 nm thick layer using EMS 150T-S before analysis. TGA-DSC is performed using STA 449 F5 Jupiter® (NETZSCH instruments) under flowing air (20 mL/min) and nitrogen (20 mL/min) at a ramp rate of 10 °C min<sup>-1</sup> from 30 to 900 °C followed by a 5 min hold at 900 °C. Galbraith laboratories performed elemental analysis using inductively coupled plasma optical emission spectrometry (ICP-OES) to determine the actual Sn, Zr, and Hf content in the samples.

### 2.3. Catalytic testing

#### 2.3.1. Kinetic testing

In a septum-sealed 10 mL two neck (2N) round-bottom flask equipped with a septum-sealed condenser, a solution (2 mL) of 0.4 M epoxide in alcohol is added with diethylene glycol dibutylether (DGDE) as the internal standard. A  $t_0$  sample (40  $\mu$ L) is drawn from this mixture before adding an amount of the catalyst to achieve an epoxide:heteroatom (Sn, Zr, or Hf) ratio of 250:1 in all tests. The round bottom flask is then lowered into a silicone oil bath pre-heated to the reaction temperature using a stir plate (600 RPM) equipped with temperature control (Heidolph). Catalytic testing demonstrates that external mass transfer does not impact the observed catalytic behavior (Fig. S1). Using a syringe-needle, 40  $\mu$ L samples are drawn at different times from the septum-sealed neck of the round bottom flask. These samples are filtered using a silica plug in a cotton-plugged glass pipette and diluted with acetone. These samples are then analyzed using Agilent 7820A GC-FID equipped with Agilent HP-5 ms Ultra Inert column. The conversion is calculated using the internal standard method. The regioselectivity is determined through comparing integrated areas of GC-FID peaks that are identified utilizing GC-MS by examining the fragmentation patterns of the species (Table S1).

#### 2.3.2. Hot-filtration test

Typical kinetic testing conditions are used to perform the hot filtration test to analyze if leached Sn atoms are responsible for the activity of Sn-Beta. After a short period of the reaction, the reaction mixture is filtered using a small 2-piece filtration apparatus. Immediately after filtration, the reaction mixture is transferred to a second 2N round bottom flask, which is subsequently immersed in a pre-heated silicone oil bath. The mixture is sampled immediately and after an extended period of reaction time to determine if further conversion of the epoxide occurs.

#### 2.3.3. Reusability testing

Reusability of the catalyst is investigated using the standard reaction of epichlorohydrin with methanol. The reactions are carried out in 50 mL 2N round bottom flasks equipped with a septum-sealed condenser. The first reaction is performed at five times the typical scale described in the kinetic testing section. After 5 h at 60 °C, the reaction mixture is allowed to cool to room temperature and filtered using a small 2-piece filtration apparatus. The filter-cake is washed with 10 mL methanol twice and then oven-dried at 80 °C overnight. The recovered catalyst is used under the same conditions, scaling the reaction contents based on the amount of catalyst recovered. This process is repeated to observe any decrease in catalyst activity or selectivity. Between the third and fourth use, the catalyst is analyzed using TGA and N<sub>2</sub> physisorption. Following calcination under conditions similar to Sn-Beta, the Sn-content is analyzed using ICP-OES, and then the material is used for the fourth time.

### 2.4. Computational methods

Density functional theory calculations are performed using the Perdew–Burke–Ernzerhof (PBE [42]) functional with D3(BJ [43]) vdW corrections, as implemented in the Vienna ab-initio Simulation Package (VASP). Starting from the BEA crystal structure from the IZA database, the energetically favorable T5 site (using notation used previously [44]) at the channel intersection is replaced by the Sn atom and is used for all calculations. For initial insights on the mechanism, the computational cost associated with evaluating different mechanisms, alcohols (i.e., methanol, n-, sec- and t-butanol) and epoxides (i.e., epichlorohydrin and propylene oxide) is reduced through performing calculations using a 5T atom cluster. The cluster is terminated by hydrogen atoms and placed in a large 24 × 24 × 26 Å<sup>3</sup> box. For a smaller subset of calculations, the predicted trends and energetics from the cluster model are verified using the full periodic structure of BEA. All calculations (both cluster and periodic) are performed using the  $\Gamma$ -point with an energy cutoff of 500 eV and a Gaussian smearing of 0.05 eV. The atomic positions are optimized until the forces are lower than 0.03 eV/Å. The transition states are determined using the climbing image nudged elastic band and the dimer method [45,46], and are verified using a vibrational analysis. All energies are referenced to adsorbed molecules within the zeolite pore.

The free energies are obtained using the harmonic approximation, where only the vibrational modes of the reacting atoms are included. This implicitly assumes that the rotational and translational modes of the long, flexible substrate molecules are decoupled with the reaction coordinate. This assumption avoids the use of the harmonic approximation for these modes [47], but may lead to underestimation of the entropy of the low frequency modes. The effect of the solvent molecules (i.e., the alcohol) is not included, which assumes that the initial and transition states in the liquid phase are stabilized to a similar extent. Although the above two assumptions may lead to deviations in the absolute value of the calculated barriers, the simplified model is expected to provide qualitative trends and insights on the reaction mechanism. Calculations examining the entropic contributions and solvent effects necessitate the use of rare event sampling [48] methods and are currently underway.

## 3. Results and discussion

### 3.1. Synthesis and characterization of catalytic materials

The Lewis acidic mesoporous and microporous materials are successfully synthesized, as demonstrated using standard characterization techniques. The PXRD data for pure Sn-Beta, Zr-Beta, and Hf-Beta are shown in Fig. S2(a) while PXRD of Sn-MFI is shown in Fig. S2(b). The data are consistent with crystalline zeolites. Analysis with nitrogen physisorption reveals that all zeolite samples (Sn-Beta, Zr-Beta, Hf-Beta, and Sn-MFI) display reversible adsorption-desorption isotherms (Type I), which is consistent with isotherm behavior for microporous materials (Fig. S3(a)). Similarly, nitrogen physisorption measurements of SBA-15, Co-Sn-SBA-15, and pure Si-SBA-15 samples display Type IV isotherms characteristic of mesoporous SBA-15 materials, as shown in Fig. S3(b). The results are listed in Table 1. Also, these materials are investigated with SEM to determine particle size (Table 1 and Fig. S4).

The materials are analyzed using elemental analysis demonstrating the successful incorporation of the desired heteroatom in the catalytic material, as shown in Table 1. Consistent with previous results, the synthesis methods achieve efficient heteroatom incorporation into the zeolite. While heteroatoms can be incorporated into the framework or form metal oxide species on the

**Table 1**  
Summary of catalysts synthesized and associated characterization data.

Material	$S_{A_{\text{physi}}} (\text{m}^2/\text{g})^{\text{a}}$	$\mu\text{pore volume} (\text{cm}^3/\text{g})^{\text{b}}$	Heteroatom (wt%) <sup>c</sup>	Si:Heteroatom	Particle size ( $\mu\text{m}$ ) <sup>d</sup>
Sn-Beta	468	0.20	0.827	237:1	$3.3 \pm 1^{\text{e}}$
Zr-Beta	432	0.18	0.597	253:1	$1.9 \pm 0.2^{\text{e}}$
Hf-Beta	432	0.18	1.91	153:1	$3.2 \pm 0.9^{\text{e}}$
Sn-MFI	407	0.14	0.773	254:1	$0.3 \pm 0.1$
Co-Sn-SBA-15	902	–	1.64	119:1	$29 \pm 12$
SBA-15 <sup>f</sup>	897	–	–	–	–
PS-Sn-SBA-15	796	–	0.921	212:1	$1.4 \pm 0.3$
Sn-Beta-re	–	–	0.763	224:1	–

<sup>a</sup> Based on nitrogen physisorption, BET method.

<sup>b</sup> Based on nitrogen physisorption, t-plot method.

<sup>c</sup> Based on elemental analysis.

<sup>d</sup> Obtained using SEM.

<sup>e</sup> Base of the bipyramidal structure noted as the largest dimension.

<sup>f</sup> Used to make PS-Sn-SBA-15.

surface, the hydrothermal methods utilized in this work are known to produce primarily framework sites. This can be demonstrated through a combination of spectroscopy methods, including DRUVS and DRIFTS. Accordingly, the zeolites are characterized using DRUVS, which has previously been used to identify the presence of  $\text{SnO}_2$ . DRUVS is used to detect the signature feature associated with  $\text{SnO}_2$ , which is observed as a shoulder around 280 nm, as shown in Fig. S5. DRUVS analysis of Sn-Beta and Sn-MFI lack this characteristic peak, suggesting that limited to no  $\text{SnO}_2$  is present in these materials.

The materials are also analyzed using DRIFTS to determine the nature of the catalytic site in the material. DRIFTS analysis of deuterated acetonitrile adsorbed onto Sn-MFI results in two peaks, as shown in Fig. S6. The peak at  $2274 \text{ cm}^{-1}$  is commonly associated with deuterated acetonitrile adsorption on a surface silanol while the peak at  $2309 \text{ cm}^{-1}$  is consistent with a framework Sn species. For Sn-Beta, DRIFTS analysis results in three distinct peaks (Fig. S6). Consistent with previous DRIFTS analysis [41], Sn-Beta has a peak at  $2282 \text{ cm}^{-1}$  associated with deuterated acetonitrile adsorption on silanols and two peaks associated with tin sites with one peak indicating open sites ( $2315 \text{ cm}^{-1}$ ) and the other peak indicative of closed sites ( $2309 \text{ cm}^{-1}$ ). The PS-Sn-SBA-15 is also analyzed with DRIFTS, revealing two peaks with one associated with silanols ( $2273 \text{ cm}^{-1}$ ) and a single weak peak around  $2306 \text{ cm}^{-1}$  that can be attributed to Sn species. Similar analysis for Zr-Beta produced a spectrum with three peaks that could be assigned to deuterated acetonitrile interacting with silanols ( $2277 \text{ cm}^{-1}$ ), closed Zr sites ( $2305 \text{ cm}^{-1}$ ) and open Zr sites ( $2312 \text{ cm}^{-1}$ ). The presence of open and closed zirconium sites is consistent with previous studies using carbon monoxide adsorption DRIFTS analysis [49]. The relative intensity of the two peaks associated with Zr sites suggests that most of the Zr sites are closed. For Hf-Beta, DRIFTS analysis reveals two peaks for deuterated acetonitrile adsorption with one peak associated with silanols ( $2275 \text{ cm}^{-1}$ ) while the other peak can be attributed to Hf species ( $2308 \text{ cm}^{-1}$ ). Recent work suggests that the hydrothermal synthesis methods results in Hf species that are open catalytic sites [50] located in the framework [51]. Overall, DRIFTS analysis indicates that the hydrothermal zeolite synthesis methods produce Lewis acidic framework catalytic sites.

### 3.2. Catalytic testing

The catalytic materials are all investigated for catalytic performance for the epoxide ring opening reaction of epichlorohydrin with methanol at  $60^\circ\text{C}$  with 0.4 mol% Sn (or the Lewis acidic heteroatom). To evaluate the effect of support characteristics, different supports (Beta, MFI, and SBA-15) substituted with tin are

investigated for catalytic activity, as shown in Fig. 1. Co-Sn-SBA-15 catalyzes the reaction, reaching  $\sim 60\%$  conversion in 24 h. While it is certainly active, all of the tin catalytic sites may not be accessible since the co-condensation synthesis method can cause the tin atoms to be incorporated into the walls of the materials. Thus, to create more accessible catalytic sites in SBA-15, Sn was incorporated post-synthetically in calcined pure Si-SBA-15 (PS-Sn-SBA-15). Compared with Co-Sn-SBA-15, PS-Sn-SBA-15 has a slight increase in catalytic activity achieving 65% in 24 h, as shown in Fig. 1. This suggests that some of the catalytic sites in Co-Sn-SBA-15 are inaccessible, but this is not a significant limitation.

While Sn-SBA-15 is active for this reaction, it is found that higher catalytic activity can be achieved through incorporating the catalytic sites in a zeolite framework. Sn-Beta is determined to be the most active material followed by Sn-MFI. The observed difference in rates between Sn-Beta and Sn-MFI could be associated with internal diffusion limitations since the smaller pore size of MFI (10 member ring; 10 MR) would have greater diffusion limitations than zeolite Beta (12 MR). Our recent work with Lewis acidic nano-MFI [52] and nano-Beta [53] zeolite synthesis demonstrates that diffusion does not affect catalytic rates for the reaction

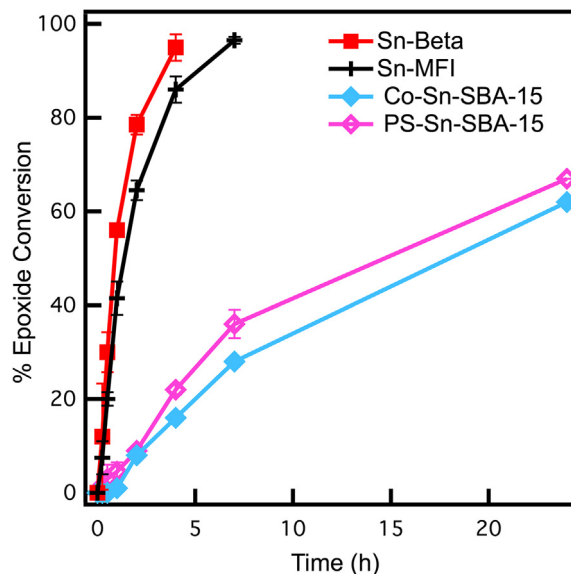


**Fig. 1.** Comparison between the catalytic performance of different catalysts, Sn-Beta (red), Sn-MFI (black), Co-Sn-SBA-15 (light blue), and PS-Sn-SBA-15 (pink), for epichlorohydrin (0.4 M) ring-opening with methanol at  $60^\circ\text{C}$  using 0.4 mol% Sn.

of epichlorohydrin with methanol, indicating that observed differences in rates are not associated with diffusion limitations.

It is investigated if the catalytic activity could be associated with SnO<sub>2</sub> species. A material incorporating SnO<sub>2</sub> into the framework is made, as described in the SI (SnO<sub>2</sub>-Beta). This material is characterized using DRUVS to demonstrate the successful incorporation of SnO<sub>2</sub>, as shown in Fig. S5c. Additionally, SnO<sub>2</sub>-Beta is tested for catalytic activity in the epoxide ring opening of epichlorohydrin with methanol. While Sn-Beta can achieve complete conversion of the epoxide in four hours, SnO<sub>2</sub>-Beta only achieves 18% conversion of the epoxide in 24 h and requires approximately two weeks to attain complete conversion (Fig. S7). These tests are consistent with the catalytic activity not being associated with amorphous SnO<sub>2</sub> species, but rather the activity being associated with framework tin.

The Lewis acidity of catalytic materials is known to strongly impact catalytic activity and selectivity. Indeed, stronger Lewis acids are beneficial for epoxide ring opening with water, but moderate strength Lewis acids such as Zr are more active than Sn for epoxide ring opening with amines [13]. Accordingly, zeolites with different Lewis acidity are investigated for the standard epoxide ring opening reaction. Both Hf-Beta and Zr-Beta are active for the epoxide ring opening reaction, as shown in Fig. 2. Compared to Sn-Beta, both Hf-Beta and Zr-Beta are less active catalysts. This can be attributed to the stronger Lewis acidity of Sn as compared to Zr and Hf, which have similar Lewis acidities [54]. This order of reactivity is in contrast with the order reported for epoxide ring opening with amines using post synthetically prepared Sn and Zr Beta [13]. On account of their higher nucleophilicity, amines bind strongly to Sn-sites lowering the reaction rates for Sn-Beta. Indeed, amines have previously been used as catalytic site poisons for Sn-Beta [55]. Being weaker nucleophiles, alcohols do not exhibit similar behavior. The stronger Lewis acidic sites result in faster rates by facilitating the nucleophilic attack.

In addition to catalytic activity, the Lewis acidic catalytic materials are highly regioselective. At complete conversion, Sn-Beta has a regioselectivity for the terminal ether (3) as determined by GC-FID analysis to be 96% (Table 2). For all Lewis acidic zeolites, the regioselectivity is consistently high. Interestingly, the regioselectivity for Al-Beta is determined to be only 93% for the terminal ether (3), indicating that the Lewis acid catalyzed mechanism is more selective than the Brønsted acid catalyzed route. Additionally, Al-Beta (epoxide:Al of 250:1; 0.4 mol% Al) only achieves greater than 90% conversion after seven hours while Sn-Beta exceeds 90% epoxide conversion in only four hours, demonstrating that Sn-Beta is more active than Al-Beta.

**Table 2**

Comparison of the catalytic performance of different catalysts analyzed in terms of turnover frequency (h<sup>-1</sup>) and regioselectivity for 3 (%) for epichlorohydrin ring opening with methanol. TOF<sub>0</sub> reported for reactions performed at 60 °C.

Material	TOF <sub>0</sub> (h <sup>-1</sup> )	Regioselectivity for 3 (%)
Sn-Beta	193	96
Sn-MFI	124	97
Hf-Beta	33	97
Zr-Beta	26	98

Sn-Beta is highly efficient for the epoxide ring opening reaction. Quantitative product yield is determined through scaling up the reaction by a factor of 10 and analyzing the reaction mixture with <sup>1</sup>H NMR with dimethyl sulfone as an NMR internal standard (Fig. S8). The yield of the terminal ether (3) is calculated to be 91%. This corroborates that Sn-Beta is a highly efficient and selective catalyst for the epoxide ring opening reaction.

Sn-Beta is highly efficient for the epoxide ring opening reaction. Quantitative product yield is determined through scaling up the reaction by a factor of 10 and analyzing the reaction mixture with <sup>1</sup>H NMR with dimethyl sulfone as an NMR internal standard (Fig. S8). The yield of the terminal ether (3) is calculated to be 91%. This corroborates that Sn-Beta is a highly efficient and selective catalyst for the epoxide ring opening reaction.

### 3.3. Reaction regioselectivity

The regioselectivity is investigated for a series of epoxides and alcohols to determine the potential scope of these catalytic materials (Fig. S9 and Table S2). Sn-Beta is used as the catalyst, unless stated otherwise. For epichlorohydrin, the regioselectivity for 3 (terminal-ether) is consistently high with values for different alcohols consistently around 97%. This spans a broad scope of alcohols, including methanol and the different butanols (1-butanol, *sec*-butanol, and *t*-butanol) tested. This indicates that the alcohol has little effect on the regioselectivity when using epichlorohydrin.

Changing the epoxide while using methanol as the nucleophile has a significant impact on the regioselectivity. Interestingly, reacting isobutylene oxide with methanol produces the terminal alcohol (4) with high regioselectivity of >99%. The identity of the regiomers is assigned through using GC-MS analysis (Table S1). Despite the steric implications of the methyl group, methanol attacks the tertiary carbon of the epoxide since this can better stabilize charge. This change in regioselectivity is consistent with the regioselectivity being controlled by inductive effects.

To further illustrate this point, two additional epoxides are tested to determine the regioselectivity: (1) epoxyoctane and (2) *n*-butyl glycidyl ether (Fig. S9). These epoxides have the same length of the backbone chain, but *n*-butyl glycidyl ether has an oxygen atom beta to the epoxide. For epoxyoctane, the regioselectivity for the terminal ether (3) is determined to be 56%. While the alkyl chain can stabilize the secondary carbocation, the effect of stabilization is insufficient to overcome the steric limitations associated with the formation of the terminal alcohol (4). For *n*-butyl glycidyl ether, the regioselectivity for the terminal ether (3) is determined to be 88%. Relative to the alkyl chain, the oxygen atom is more electronegative than a carbon atom, reducing the stability of the 2 position relative to the terminal carbon. Overall, the observed regioselectivity can be attributed to the inductive effect of the functional groups in the vicinity of the epoxide. This suggests that the zeolite beta framework is beneficial to increase the catalytic rate, but it has little to no impact on the regioselectivity for the epoxides and alcohols that are tested in this work. To investigate if the heteroatom in zeolite Beta affects regioselectivity, Sn-Beta, Hf-Beta, and Zr-Beta are analyzed for ring opening of

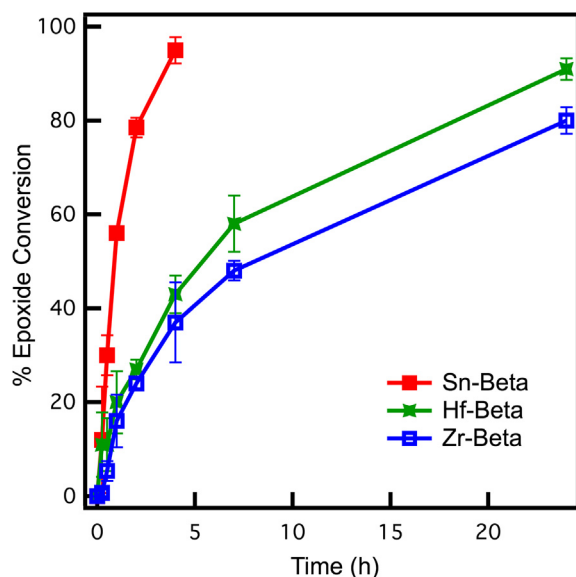


**Fig. 2.** Comparison of the catalytic performance of zeolite beta catalysts with different heteroatoms, Sn-Beta (red), Zr-Beta (blue), and Hf-Beta (green) for epichlorohydrin (0.4 M) ring-opening with methanol at 60 °C using 0.4 mol% Lewis acid.

1,2-epoxybutane with methanol. The regioselectivity shows a modest increase from 54% to 56% to 60% for Sn-Beta, Hf-Beta, and Zr-Beta respectively (Fig. S9(e)).

### 3.4. Catalyst stability and reusability

The robustness of Sn-Beta is evaluated through a combination of a hot-filtration test and catalyst reuse experiments. Recent reports indicate deactivation of Sn-Beta in biomass conversion reactions through leaching of tin species [56,57]. In addition to decreasing the reusability of these materials, the leached Sn species may be responsible for catalytic activity. Therefore, the propensity for Sn sites to leach is evaluated for the standard epoxide ring opening reaction with methanol using a hot filtration test. After 30 min of reaction time, the catalyst is filtered from the reaction mixture using a two-piece filtration apparatus. The filtrate is transferred to a round-bottom flask and allowed to react at 60 °C, taking samples periodically to determine the conversion over time. As shown in Fig. 3, the epoxide conversion effectively stops after the catalyst is removed from the mixture. These results provide evidence that homogeneous species are not responsible for the catalytic activity and that the catalytic site does not leach from the material. Additionally, these results indicate that the catalytic site is likely a framework species, suggesting that the material could be a robust and reusable catalyst for this reaction.

The reusability of Sn-Beta for the epoxide ring opening reaction is examined through recycling the catalyst for three catalytic tests using the standard epoxide ring opening reaction. For the first test, the reaction is scaled to five times the typical reaction volume to ensure sufficient material could be recovered for multiple reuse tests. Samples are withdrawn periodically to determine conversion over time, as shown in Fig. 4. After five hours of reaction, the reaction is stopped through removing the round-bottom flask from the silicone oil bath. The reaction mixture is filtered, the catalyst washed, dried, and weighed to determine the amount of catalyst recovered, and the second cycle is performed through scaling the amount of reaction mixture to the amount of catalyst to maintain 0.4 mol% Sn (epoxide:Sn of 250:1). As shown in Fig. 4, the conversion is nearly identical for the first, second, and third cycle, indicat-

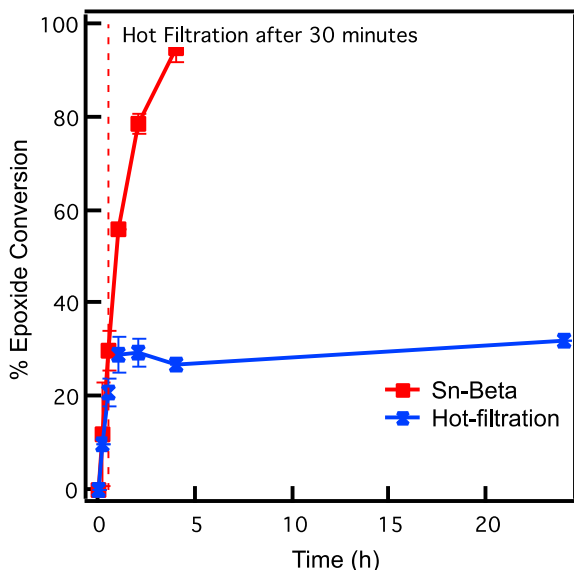


Fig. 3. Hot filtration test for Sn-Beta in the epoxide ring opening reaction of epichlorohydrin with methanol at 60 °C using 0.4 mol% Sn. The conversion is shown as a function of time for the standard Sn-Beta (red) test and the Sn-Beta hot-filtration test (blue). Hot filtration is performed at 30 min (marked by dotted line).

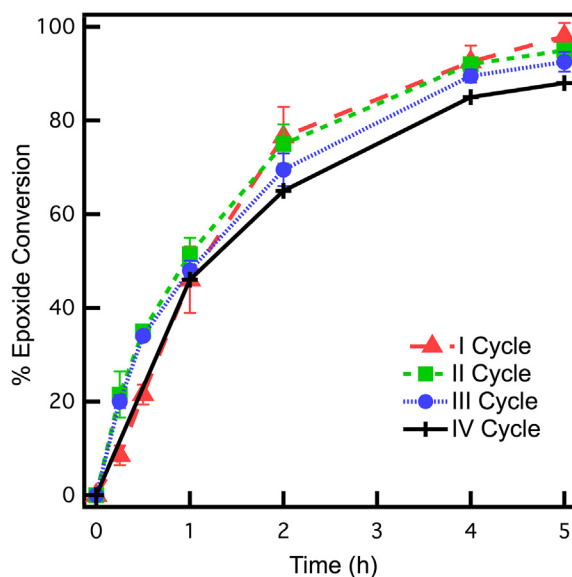


Fig. 4. Comparison between fresh (red), once used (green), and twice used (blue) Sn-Beta for epichlorohydrin ring opening with methanol shows no significant differences in activity. Same can be concluded for the calcined twice used catalyst (black).

ing that the catalytic material can be readily reused without loss of catalytic activity. After the third cycle, the catalyst is recovered through filtration, calcined, and is analyzed for elemental composition. Elemental analysis (EA) reveals a decrease in the weight percentage of Sn from 0.827% to 0.763%. This difference is small compared to the expected accuracy of EA. At the same time, the Sn:Si does not change significantly from 237:1 before reaction to 224:1 after 3 cycles, indicating that the catalytic material remains robust. Using the catalyst for a fourth time (labeled Sn-Beta-re in Table 1) reveals that the catalytic activity is maintained even in a fourth cycle. Combined these results indicate that Sn-Beta is a promising and reusable catalyst for the epoxide ring opening reaction with alcohols.

### 3.5. Catalytic reaction mechanism from DFT calculations

Inspired by the promising experimental results, DFT calculations are used to further understand the reaction mechanism. As summarized in Fig. 5 and S11, three potential reaction mechanisms involving a single alcohol and epoxide molecule are explored: (1) activation of the epoxide by an alcohol that is dissociated and bound to the Sn site; (2) activation of the epoxide by an alcohol that is intact and bound to the Sn site; and (3) activation of the epoxide bound by the Sn site for attack by the alcohol. In addition to mechanisms involving a single alcohol, a mechanism is considered that involves the  $S_N2$ -type activation of the epoxide by a Sn-bound alcohol and simultaneous nucleophilic attack by a 2nd alcohol molecule. Each of these mechanisms involve several steps, including the adsorption of the substrate on the catalytic site and the coupling reaction. Using the periodic BEA model, the binding energy is calculated for non-dissociative adsorption of methanol and epichlorohydrin (<5 kJ/mol difference; see SI and Fig. S11 for details). Similar calculations for water and ethanol dissociation using a different functional and more sophisticated methods have been recently reported for ethanol dehydration [47] that indicate that the interaction energies for water and ethanol with the catalytic site are similar. Accordingly, these calculations indicate that the experimental conditions employed in these studies (i.e., 0.4 M epoxide in alcohol) would result in the catalytic sites to be

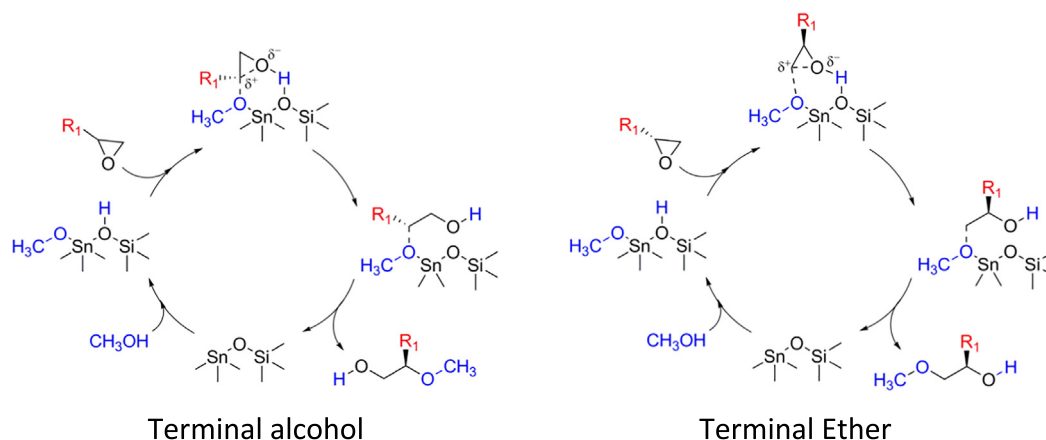


Fig. 5. Activation of the epoxide by an alcohol that is dissociated and bound to the Sn site (Mechanism 1).

interacting with the alcohol. Even small amounts of water that might be present in the hydrophobic framework would be expected to be displaced from the catalytic site by methanol.

In addition to intact binding of substrates, the energy of the transition state is calculated for dissociation of methanol and epichlorohydrin over the Sn-site (Fig. S12). The calculated free energy barrier for methanol dissociation ( $\Delta G_{\text{methanol,diss}}^a = 53$  kJ/mol) is significantly lower than the corresponding value for epichlorohydrin ( $\Delta G_{\text{epichlorohydrin,diss}}^a = 135$  kJ/mol). The experimentally calculated activation energy ( $53 \pm 7$  kJ/mol; details in SI and Fig. S13) is significantly lower than  $\Delta G_{\text{epichlorohydrin,diss}}^a$ , indicating that the dominant reaction pathway does not involve the dissociative adsorption of the epoxide. For all these different mechanisms, the rate determining step involves the reaction between the alcohol and the epoxide and the activation barrier is associated with breaking the  $\text{C}_{\text{epoxide}}-\text{O}_{\text{epoxide}}$  bond.

The activation barrier for  $\text{C}_{\text{epoxide}}-\text{O}_{\text{epoxide}}$  bond breaking is examined for the different mechanisms for the reaction between methanol and epichlorohydrin. Table 3 summarizes the free energy barriers for the rate determining step of the four mechanisms (transition states shown in Figs. S14–S19). The calculated barriers for intact, bound methanol ( $\Delta G_{\text{intact,bound alcohol}}^a = 137 - 155$  kJ/mol, mechanism 2) and bound epoxide ( $\Delta G_{\text{bound epoxide}}^a = 114 - 120$  kJ/mol, mechanism 3) pathways are higher than the dissociated methanol ( $\Delta G_{\text{dissociated,bound alcohol}}^a = 76 - 82$  kJ/mol, mechanism 1) and two methanol  $\text{S}_{\text{N}}2$  pathway ( $\Delta G_{\text{two alcohol,SN2}}^a = 74 - 62$  kJ/mol, mechanism 4). The high barrier for the intact, bound alcohol pathway (mechanism 3) arises because of the strained transition state geometry and is not discussed further as it is associated with an inaccessible reaction barrier at reaction conditions. The relative excess of the alcohol compared to the epoxide (i.e., 0.4 M) and the similar binding energies of the epoxide and the alcohol to the Sn site (difference  $< 5$  kJ/mol) suggest that only a small fraction of the Sn sites will be epoxide bound. Here, the low coverage of

the epoxide along with higher calculated barriers (compared to mechanism 1 and 4) indicate a negligible contribution of the bound epoxide mechanism (mechanism 2).

At this stage, it is useful to compare mechanism 1 and 4 in more detail, especially as they relate to the observed regioselectivity. The regioselectivity is determined by which  $\text{C}_{\text{epoxide}}-\text{O}_{\text{epoxide}}$  bond is cleaved during the reaction. Thus, calculations are performed examining both modes of breaking the  $\text{C}_{\text{epoxide}}-\text{O}_{\text{epoxide}}$  bond. To reduce the computational cost, a 5T cluster model are used for the following analysis. The two epoxides considered are epichlorohydrin and isobutylene oxide since these epoxides provide distinct regioselectivities. For epichlorohydrin, nucleophilic attack at the primary  $\text{C}_{\text{epoxide}}$  leads to the terminal ether product ( $\sim 97\%$ ), while attack at the secondary C leads to the minor terminal alcohol product ( $\sim 3\%$ ). Mechanism 1 involves protonation of the  $\text{O}_{\text{epoxide}}$  by the dissociated methanol, followed by front-side  $\text{S}_{\text{N}}1$ -type nucleophilic attack on the  $\text{C}_{\text{epoxide}}$ . As with  $\text{S}_{\text{N}}1$  reactions, a lower barrier (76 kJ/mol) is observed for the formation of the more stable, secondary carbocation compared to the primary carbocation (82 kJ/mol) pathway. In contrast, the trends for the  $\text{S}_{\text{N}}2$ , mechanism 4 are reversed, where the lowest barrier (62 kJ/mol) is observed for reaction at the primary  $\text{C}_{\text{epoxide}}$  as determined by the low steric hindrance. Thus, results from epichlorohydrin/methanol are consistent with the two alcohol,  $\text{S}_{\text{N}}2$  mechanism (mechanism 4) involving nucleophilic attack of the less sterically hindered primary  $\text{C}_{\text{epoxide}}$  being responsible for the experimentally observed regioselectivity for the terminal ether product for the epichlorohydrin/methanol reaction.

From the above discussion, it is clear that the experimentally observed regioselectivity depends on the energetics of the  $\text{S}_{\text{N}}1$  and  $\text{S}_{\text{N}}2$  pathway for the reactant epoxide. To examine this hypothesis further, a similar analysis is performed for the reaction between isobutylene oxide and methanol. In contrast to the epichlorohydrin results above, the reaction of isobutylene oxide and methanol results exclusively in the terminal alcohol ( $\sim 100\%$ )

Table 3  
DFT-calculated activation free energies (at 80 °C) for the reaction of epichlorohydrin with methanol for different mechanisms.

Product	Terminal alcohol	Terminal ether
Reaction site	Secondary $\text{C}_{\text{epoxide}}$	Primary $\text{C}_{\text{epoxide}}$
Mechanism 1	76	82
Mechanism 2	137	155
Mechanism 3	114	120
Mechanism 4	74	62

Table 4  
DFT-calculated activation free energies (at 80 °C) for the reaction of isobutylene oxide with methanol for different mechanisms.<sup>a</sup>

Product	Terminal alcohol	Terminal ether
Reaction site	Tertiary $\text{C}_{\text{epoxide}}$	Primary $\text{C}_{\text{epoxide}}$
Mechanism 1	61	92
Mechanism 4	73	72

<sup>a</sup> Mechanism 2 and 3 are not evaluated for this reaction because of the high barriers calculated previously for epichlorohydrin and methanol for these mechanisms.

regiomer, which arises because of the nucleophilic attack at the tertiary C<sub>epoxide</sub>. The calculated free energy barriers for mechanism 1 and mechanism 4 are presented in Table 4. For the reaction occurring at the tertiary C<sub>epoxide</sub>, it is observed that S<sub>N</sub>1 mechanism (61 kJ/mol, mechanism 1) is preferred compared to the S<sub>N</sub>2 pathway (73 kJ/mol, mechanism 4) owing to the higher stability of the tertiary carbocation. Further, the S<sub>N</sub>1 pathway is not favored for the primary carbocation (92 kJ/mol) and a S<sub>N</sub>2 pathway (72 kJ/mol) is preferred. Thus, in the case of isobutylene oxide, it can be concluded that the high steric hindrance at the tertiary C<sub>epoxide</sub> along with the stability of a tertiary carbocation leads to S<sub>N</sub>1 mechanism 1 as the dominant reaction pathway. Consistent with the experimental trends, this leads to the formation of the terminal alcohol product.

Although the trends predicted by the above mechanistic analysis are consistent with experimental observations, it is acknowledged that the computational results (1) are based on small energy differences (<20 kJ/mol) and (2) involve significant assumptions related to the position and nature of the Sn-site, the entropic contributions, and the possible solvent effects. Using the DFT calculated energy barriers and rate constants, preliminary calculations (see SI for details) show that these small energy differences can explain the experimentally observed high selectivity. Moreover, the experimental activation energy (53 ± 7 kJ/mol, calculated from kinetic experiments at different temperatures) is most similar to the barrier associated with mechanism 1 and 4 (~61–62 kJ/mol), which supports our conclusions regarding the dominant mechanism. Further detailed calculations based on rare-event sampling methods are currently underway, but these calculations are beyond the scope of this first report of Sn-zeolites as active catalysts for alcohol ring opening reaction.

#### 4. Summary

Lewis acidic materials are determined to be regioselective catalysts for epoxide ring opening of epichlorohydrin with alcohols. Of the mesoporous and microporous materials tested, kinetic testing demonstrated that Sn-Beta has a higher catalytic activity than other Sn, Hf, and Zr-substituted materials. For epichlorohydrin ring opening with methanol, Sn-Beta is more active and achieves a higher regioselectivity than Al-Beta. The regioselectivity is primarily associated with the epoxide and not the nucleophile nor the material pore size. Indeed, the results for regioselectivity for most cases across a broad range of epoxides is consistent with the inductive effect. The activation energy for epichlorohydrin and methanol is determined to be 53 ± 7 kJ/mol. This reaction barrier is consistent with DFT calculations of a mechanism that involves two alcohols acting in concert with one alcohol adsorbed on the catalytic site that activates the epoxide and the second alcohol opening the epoxide. DFT calculations indicate that the mechanism depends on the epoxide since alcohol ring opening of isobutylene oxide is calculated to involve alcohol activation on the Lewis acidic site with the rate limiting step associated with the epoxide ring opening step. Importantly, Sn-Beta is a reusable and selective catalyst for epoxide ring opening with alcohols, as demonstrated for epichlorohydrin ring opening with methanol.

#### Acknowledgements

We gratefully acknowledge the American Chemical Society Petroleum Research Fund (ACS-PRF 55946-DNI5), the National Science Foundation (NSF Career 1653587), and the Ohio State University Institute for Materials Research (OSU IMR FG0138) for their financial support. This research used resources of the National Energy Research Scientific Computing Center (NERSC), a U.S. Department

of Energy Office of Science User Facility operated under Contract No. DE-AC02-05CH11231. We thank Prof. Justin Notestein and Mihir Bhagat from Northwestern University for providing insightful discussion and samples for comparative analysis to facilitate identification of different regiomers.

#### Appendix A. Supplementary material

Supplementary data to this article can be found online at <https://doi.org/10.1016/j.jcat.2018.11.038>.

#### References

- [1] B. Tang, W. Dai, G. Wu, N. Guan, L. Li, M. Hunger, Improved postsynthesis strategy to Sn-beta zeolites as lewis acid catalysts for the ring-opening hydration of epoxides, *ACS Catal.* 4 (2014) 2801–2810, <https://doi.org/10.1021/cs500891s>.
- [2] M. Tokunaga, J.F. Larrow, F. Kakiuchi, E.N. Jacobsen, Asymmetric catalysis with water: Efficient kinetic resolution of terminal epoxides by means of catalytic hydrolysis, *Science* 277 (1997) 936–938, <https://doi.org/10.1126/science.277.5328.936>.
- [3] S.S. Kahandal, S.R. Kale, S.T. Disale, R.V. Jayaram, Sulphated yttria-zirconia as a regioselective catalyst system for the alcoholysis of epoxides, *Catal. Sci. Technol.* 2 (2012) 1493–1499, <https://doi.org/10.1039/c2cy20116j>.
- [4] D.B.G. Williams, M. Lawton, Aluminium triflate: a remarkable Lewis acid catalyst for the ring opening of epoxides by alcohols, *Org. Biomol. Chem.* 3 (2005) 3269–3272, <https://doi.org/10.1039/b508924g>.
- [5] M. Mirza-aghayan, M. Alizadeh, M. Molaee, R. Boukherroub, Graphite oxide: a simple and efficient solid acid catalyst for the ring-opening of epoxides by alcohols, *Tetrahedron Lett.* 55 (2014) 6694–6697, <https://doi.org/10.1016/j.tetlet.2014.10.050>.
- [6] J. Otera, Y. Yoshinaga, K. Hirakawa, Highly regioselective ring opening of epoxides with alcohols catalyzed by organotin phosphate condensates, *Tetrahedron Lett.* 26 (1985) 3219–3222.
- [7] M. Chini, P. Crotti, C. Gardelli, F. Macchia, Metal salt-promoted alcoholysis of 1,2-Epoxides, *Synlett* (1992) 673–676, <https://doi.org/10.1055/s-1992-21454>.
- [8] C. Wang, L. Luo, H. Yamamoto, Metal-catalyzed directed regio- and enantioselective ring-opening of epoxides, *Acc. Chem. Res.* 49 (2016) 193–204, <https://doi.org/10.1021/acs.accounts.5b00428>.
- [9] Y. Liu, R.C. Klet, J.T. Hupp, O. Farha, Probing the correlations between the defects in metal-organic frameworks and their catalytic activity by an epoxide ring-opening reaction, *Chem. Commun.* 52 (2016) 7806–7809, <https://doi.org/10.1039/C6CC03727E>.
- [10] Y. Feng, M.E. Lydon, C.W. Jones, Polymer resin supported cobalt-salen catalysts: Role of Co(II) salen species in the regioselective ring opening of 1,2-epoxyhexane with methanol, *ChemCatChem.* 5 (2013) 3636–3643, <https://doi.org/10.1002/cctc.201300578>.
- [11] B.H. Kim, F. Piao, E.J. Lee, J.S. Kim, Y.M. Jun, B.M. Lee, InCl<sub>3</sub>-catalyzed regioselective ring-opening reactions of epoxides to beta-hydroxy ethers, *Bull. Korean Chem. Soc.* 25 (2004) 881–888, <https://doi.org/10.5012/bkcs.2004.25.6.881>.
- [12] N.E. Thornburg, Y. Liu, P. Li, J.T. Hupp, O.K. Farha, J.M. Notestein, MOFs and their grafted analogues: regioselective epoxide ring-opening with Zr 6 nodes, *Catal. Sci. Technol.* 6 (2016) 6480–6484, <https://doi.org/10.1039/C6CY01093H>.
- [13] B. Tang, W. Dai, X. Sun, G. Wu, N. Guan, M. Hunger, L. Li, Mesoporous Zr-Beta zeolites prepared by a post-synthetic strategy as a robust Lewis acid catalyst for the ring-opening aminolysis of epoxides, *Green Chem.* 17 (2015) 1744–1755, <https://doi.org/10.1039/C4GC02116A>.
- [14] N. Azizi, M.R. Saidi, Highly chemoselective addition of amines to epoxides in water, *Org. Lett.* 7 (2005) 3649–3651, <https://doi.org/10.1021/ol051220q>.
- [15] T. Baskaran, A. Joshi, G. Kamalakar, A. Sakthivel, A solvent free method for preparation of beta-amino alcohols by ring opening of epoxides with amines using MCM-22 as a catalyst, *Appl. Catal. A Gen.* 524 (2016) 50–55, <https://doi.org/10.1016/j.apcata.2016.05.029>.
- [16] H. Takeuchi, K. Kitajima, Y. Yamamoto, K. Mizuno, The use of proton-exchanged X-type zeolite in catalyzing ring-opening reactions of 2-substituted epoxides with nucleophiles and its effect on regioselectivity, *J. Chem. Soc. Trans.* 2 (1993) 199–203, <https://doi.org/10.1039/p29930000199>.
- [17] V. Mirkhani, S. Tangestaninejad, B. Yadollahi, L. Alipanah, Efficient regio- and stereoselective ring opening of epoxides with alcohols, acetic acid and water catalyzed by ammonium decatungstate(IV), *Tetrahedron* 59 (2003) 8213–8218, <https://doi.org/10.1016/j.tet.2003.08.018>.
- [18] W.A. Nugent, Chiral lewis acid catalysis. Enantioselective addition of azide to meso epoxides, *J. Am. Chem. Soc.* 114 (1992) 2768–2769, <https://doi.org/10.1021/ja00033a090>.
- [19] R. Munirathinam, D. Joe, J. Huskens, W. Verboom, Regioselectivity control of the ring opening of epoxides with sodium azide in a microreactor, *J. Flow Chem.* 2 (2012) 129–134, <https://doi.org/10.1556/JFC-D-12-00013>.
- [20] G.D. Yadav, P.S. Surve, Regioselective ring opening reaction of epichlorohydrin with acetic acid to 3-chloro-2-hydroxypropyl acetate over cesium modified heteropolyacid on clay support, *Appl. Catal. A Gen.* 468 (2013) 112–119, <https://doi.org/10.1016/j.apcata.2013.08.003>.

- [21] Dow Chemical, Dowanol TM PM, 7 (2012) 1–6. <http://www.dow.com/en-us/markets-and-solutions/products/Dowanol/DowanolPMGlycolEther>.
- [22] M.P. Kirkup, R. Rizvi, B.B. Shankar, S. Dugar, J.W. Clader, S.W. McCombie, S.I. Lin, N. Yumibe, K. Huie, M. Van Heek, D.S. Compton, H.R. Davis, A.T. McPhail, (-)-SCH 57939: Synthesis and pharmacological properties of a potent, metabolically stable cholesterol absorption inhibitor, *Bioorganic Med. Chem. Lett.* 6 (1996) 2069–2072, [https://doi.org/10.1016/0960-894X\(96\)00365-4](https://doi.org/10.1016/0960-894X(96)00365-4).
- [23] X. Hu, J. Fan, C.Y. Yue, Ring-opening polymerization of epichlorohydrin and its copolymerization with other alkylene oxides by quaternary catalyst system, *J. Appl. Polym. Sci.* 80 (2001) 2446–2454, <https://doi.org/10.1002/app.1351>.
- [24] H. Ogawa, Y. Miyamoto, T. Fujigaki, T. Chihara, Ring-opening of 1,2-epoxyalkane with alcohols over H-ZSM-5 in liquid phase, *Catal. Letters.* 40 (1996) 253–255, <https://doi.org/10.1007/BF00815291>.
- [25] G.A. Olah, A.P. Fung, D. Meidar, *Synthetic methods and reactions*; 68 1. Nafion-H-catalyzed hydration and methanolysis of epoxides, *Synthesis (Stuttg)* (1981) 280–282, <https://doi.org/10.1055/s-1981-29414>.
- [26] N.A. Brunelli, W. Long, K. Venkatasubbaiah, C.W. Jones, Catalytic regioselective epoxide ring opening with phenol using homogeneous and supported analogues of dimethylaminopyridine, *Top. Catal.* 55 (2012) 432–438, <https://doi.org/10.1007/s11244-012-9822-2>.
- [27] A. Dhakshinamoorthy, M. Alvaro, H. Garcia, Metal-organic frameworks as efficient heterogeneous catalysts for the regioselective ring opening of epoxides, *Chem. - A Eur. J.* 16 (2010) 8530–8536, <https://doi.org/10.1002/chem.201000588>.
- [28] D.E. White, P.M. Tadross, Z. Lu, E.N. Jacobsen, A broadly applicable and practical oligomeric (salen)Co catalyst for enantioselective epoxide ring-opening reactions, *Tetrahedron* 70 (2014) 4165–4180, <https://doi.org/10.1016/j.tet.2014.03.043>.
- [29] X. Zhu, K. Venkatasubbaiah, M. Weck, C.W. Jones, Highly active oligomeric Co (salen) catalysts for the asymmetric synthesis of *α*-aryloxy or *α*-alkoxy alcohols via kinetic resolution of terminal epoxides, *J. Mol. Catal. A Chem.* 329 (2010) 1–6, <https://doi.org/10.1016/j.molcata.2010.06.015>.
- [30] L.E. Martinez, J.L. Leighton, D.H. Carsten, E.N. Jacobsen, Highly enantioselective ring opening of epoxides catalyzed by (salen)Cr(III) complexes, *J. Am. Chem. Soc.* 117 (1995) 5897–5898, <https://doi.org/10.1021/ja00126a048>.
- [31] E.N. Jacobsen, Asymmetric catalysis of epoxide ring-opening reactions, *Acc. Chem. Res.* 33 (2000) 421–431, <https://doi.org/10.1021/ar960061v>.
- [32] A. Corma, L. Nemeth, M. Renz, S. Valencia Valencia, Sn-zeolite beta as a heterogeneous chemoselective catalyst for Baeyer-Villiger oxidations, *Nature* 412 (2001) 423–425.
- [33] A. Corma, M.E. Domine, L. Nemeth, S. Valencia Valencia, Al-free Sn-Beta zeolite as a catalyst for the selective reduction of carbonyl compounds (Meerwein-Ponndorf-Verley reaction), *J. Am. Chem. Soc.* 124 (2002) 3194–3195.
- [34] M. Moliner, Y. Roman-Leshkov, M.E. Davis, Tin-containing zeolites are highly active catalysts for the isomerization of glucose in water, *Proc. Natl. Acad. Sci.* 107 (2010) 6164–6168, <https://doi.org/10.1073/pnas.1002358107>.
- [35] J.J. Pacheco, M.E. Davis, Synthesis of terephthalic acid via Diels-Alder reactions with ethylene and oxidized variants of 5-hydroxymethylfurfural, *Proc. Natl. Acad. Sci. USA* 111 (2014) 8363–8367, <https://doi.org/10.1073/pnas.1408345111>.
- [36] V. Ramaswamy, P. Shah, K. Lazar, A.V. Ramaswamy, Synthesis, characterization and catalytic activity of Sn-SBA-15 mesoporous molecular sieves, *Catal. Surv. from Asia.* 12 (2008) 283–309, <https://doi.org/10.1007/s10563-008-9060-6>.
- [37] N. Deshpande, L. Pattanaik, M.R. Whitaker, C. Yang, L. Lin, N.A. Brunelli, Selectively converting glucose to fructose using immobilized tertiary amines, *J. Catal.* 353 (2017) 205–210, <https://doi.org/10.1016/j.jcat.2017.07.021>.
- [38] Q. Huo, D.I. Margolese, G.D. Stucky, Surfactant control of phases in the synthesis of mesoporous silica-nased materials, *Chem. Mater.* 4756 (1996) 1147–1160, <https://doi.org/10.1021/cm960137h>.
- [39] S. Valencia Valencia, A. Corma, Stannosilicate molecular sieves, 1999.
- [40] R. Bermejo-Deval, R. Gounder, M.E. Davis, Framework and extraframework tin sites in zeolite beta react glucose differently, *ACS Catal.* 2 (2012) 2705–2713, <https://doi.org/10.1021/cs300474x>.
- [41] S. Roy, K. Bakhmutsky, E. Mahmoud, R.F. Lobo, R.J. Gorte, Probing lewis acid sites in Sn-Beta zeolite, *ACS Catal.* 3 (2013) 573–580, <https://doi.org/10.1021/cs300599z>.
- [42] J.P. Perdew, K. Burke, M. Ernzerhof, Generalized gradient approximation made simple, *Phys. Rev. Lett.* 77 (1996) 3865–3868, <https://doi.org/10.1103/PhysRevLett.77.3865>.
- [43] B.R. Brooks, C.L. Brooks III, A.D. Mackerell Jr., L. Nilsson, R.J. Petrella, B. Roux, Y. Won, G. Archontis, C. Bartels, S. Boresch, A. Caffisch, L. Caves, Q. Cui, A.R. Dinner, M. Feig, S. Fischer, J. Gao, M.W.I. Hodoscek, M. Karplus, Effect of the damping function in dispersion corrected density functional theory, *J. Comput. Chem.* 32 (2011) 1456–1465, <https://doi.org/10.1002/jcc>.
- [44] J.M. Newsam, M.M.J. Treacy, W.T. Koetsier, C.B. de Gruyter, *Structural characterization of zeolite beta*, *Proc. R. Soc. A.* 420 (1988) 375–405.
- [45] G. Henkelman, H. Jónsson, A dimer method for finding saddle points on high dimensional potential surfaces using only first derivatives, *J. Chem. Phys.* 111 (1999) 7010–7022, <https://doi.org/10.1063/1.1329672>.
- [46] G. Henkelman, B.P. Uberuaga, H. Jónsson, Climbing image nudged elastic band method for finding saddle points and minimum energy paths, *J. Chem. Phys.* 113 (2000) 9901–9904, <https://doi.org/10.1063/1.1329672>.
- [47] B.C. Bukowski, J.S. Bates, R. Gounder, J. Greeley, First principles, microkinetic, and experimental analysis of Lewis acid site speciation during ethanol dehydration on Sn-Beta zeolites, *J. Catal.* 365 (2018) 261–276, <https://doi.org/10.1016/j.jcat.2018.07.012>.
- [48] V. Van Speybroeck, J. Van Der Mynsbrugge, M. Vandichel, K. Hemelsoet, D. Lesthaeghe, A. Ghysels, G.B. Marin, M. Waroquier, First principle kinetic studies of zeolite-catalyzed methylation reactions, *J. Am. Chem. Soc.* 133 (2011) 888–899, <https://doi.org/10.1021/ja1073992>.
- [49] V.L. Sushkevich, A. Vimont, A. Travert, I.I. Ivanova, Spectroscopic evidence for open and closed lewis acid sites in ZrBEA zeolites spectroscopic evidence for open and closed lewis acid sites in ZrBEA zeolites, *J. Phys. Chem. C* 119 (2015) 17633–17639, <https://doi.org/10.1021/acs.jpcc.5b02745>.
- [50] Y. Wang, J.D. Lewis, Y. Roman-Leshkov, Synthesis of itaconic acid ester analogues via self-aldol condensation of ethyl pyruvate catalyzed by hafnium BEA zeolites, *ACS Catal.* 6 (2016) 2739–2744, <https://doi.org/10.1021/acscatal.6b00561>.
- [51] T. Iida, K. Ohara, Y. Roman-Leshkov, T. Wakihara, Zeolites with isolated-framework and oligomeric-extraframework hafnium species characterized with pair distribution function analysis, *Phys. Chem. Chem. Phys.* 20 (2018) 7914–7919, <https://doi.org/10.1039/c8cp00464a>.
- [52] A. Parulkar, R. Joshi, N. Deshpande, N.A. Brunelli, Synthesis and catalytic testing of lewis acidic nano-MFI zeolites for the epoxide ring opening reaction with alcohol, *Appl. Catal. A, Gen.* 566 (2018) 25–32, <https://doi.org/10.1016/j.apcata.2018.08.018>.
- [53] A. Parulkar, A. Spanos, N. Deshpande, N.A. Brunelli, Lewis acidic nano zeolite beta for epoxide ring opening with alcohols (in preparation), (n.d.).
- [54] W.R. Gunther, V.K. Michaelis, R.G. Griffin, Y. Román-Leshkov, Interrogating the lewis acidity of metal sites in beta zeolites with 15 N pyridine adsorption coupled with MAS NMR spectroscopy, *J. Phys. Chem. C* 120 (2016) 28533–28544.
- [55] J.W. Harris, M.J. Cordon, J.R. Di Iorio, J.C. Vega-Vila, F.H. Ribeiro, R. Gounder, Titration and quantification of open and closed Lewis acid sites in Sn-Beta zeolites that catalyze glucose isomerization, *J. Catal.* 335 (2016) 141–154, <https://doi.org/10.1016/j.jcat.2015.12.024>.
- [56] N. Rajabbeigi, A.I. Torres, C.M. Lew, B. Elyassi, L. Ren, Z. Wang, H. Je Cho, W. Fan, P. Daoutidis, M. Tsapatsis, On the kinetics of the isomerization of glucose to fructose using Sn-Beta, *Chem. Eng. Sci.* 116 (2014) 235–242, <https://doi.org/10.1016/j.ces.2014.04.031>.
- [57] G.M. Lari, P.-Y. Dapsens, D. Scholz, S.G. Mitchell, C. Mondelli, J. Pérez-Ramírez, Deactivation mechanisms of tin-zeolites in biomass conversions, *Green Chem.* 18 (2016) 1249–1260, <https://doi.org/10.1039/C5GC02147B>.